

# FedGA: Federated Learning with Gradient Alignment for Error Asymmetry Mitigation

Chenguang Xiao, Zheming Zuo\*, Shuo Wang

School of Computer Science, University of Birmingham, UK  
cxx075@student.bham.ac.uk, {z.zuo.1, s.wang.2}@bham.ac.uk

## Abstract

Federated learning (FL) triggers intra-client and inter-client class imbalance, with the latter compared to the former leading to biased client updates and thus deteriorating the distributed models. Such a bias is exacerbated during the server aggregation phase and has yet to be effectively addressed by conventional re-balancing methods. To this end, different from the off-the-shelf label or loss-based approaches, we propose a gradient alignment (GA)-informed FL method, dubbed as FedGA, where the importance of error asymmetry (EA) in bias is observed and its linkage to the gradient of the loss to raw logits is explored. Concretely, GA, implemented by label calibration during the model backpropagation process, prevents catastrophic forgetting of rare and missing classes, hence boosting model convergence and accuracy. Experimental results on five benchmark datasets demonstrate that GA outperforms the pioneering counterpart FedAvg and its four variants in minimizing EA and updating bias, and accordingly yielding higher F1 score and accuracy margins when the Dirichlet distribution sampling factor  $\alpha$  increases. The code and more details are available at <https://anonymous.4open.science/r/FedGA-B052/README.md>.

## Introduction

Federated learning (FL) utilizes data stored on edge devices to enable knowledge extraction (Zhang et al. 2024) from distributed data while maintaining privacy (Zuo et al. 2021). However, FL faces significant challenges due to data heterogeneity (Shi et al. 2024; Wang et al. 2024c), particularly class imbalance (Wu et al. 2024), where classes are unequally represented in the training data. Class imbalance issues are prevalent in various real-world applications, including online grooming detection (Zuo et al. 2019), clinical diagnosis (Wu et al. 2023), brand anti-counterfeiting (Zuo et al. 2024) etc. Noteworthy, FL deployed in distributed agents tend to enhance model performance with privacy preserved (Yazdinejad et al. 2024), yet class imbalance issues can hinder minority class prediction precision and slow model convergence (Wang et al. 2024b).

Class imbalance in FL typically manifests as intra-client and inter-client imbalances (Shen et al. 2021; Wang et al.

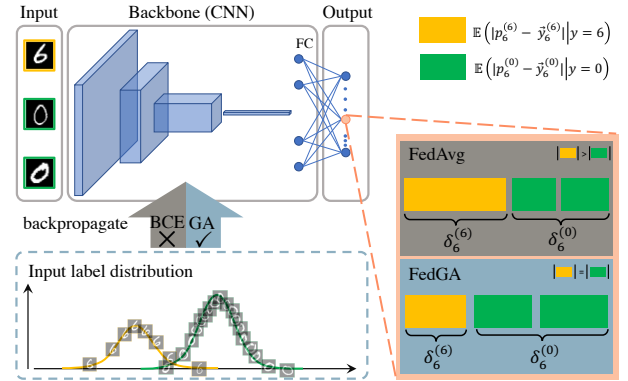


Figure 1: We propose an FL framework for error asymmetry mitigation caused by class imbalance. Our gradient alignment (GA) method, different from binary cross entropy (BCE) adopted in the prestigious FedAvg, scales active and inactive gradients through the label calibration to guide the model backpropagation process, thus reducing client update bias and allaying privacy and communication concerns.

2021; Pei et al. 2024). The former analogizes the traditional class imbalance in centralized learning (CL), and the latter refers to mismatched class distributions between clients, *e.g.* one client having only class 0 data and another having only class 1 data, adding complexity to the issue. The investigation of inter-client class imbalance is nascent. Conventional re-balancing techniques, *e.g.* oversampling and undersampling from CL, are often ineffective due to system constraints (Xiao and Wang 2023), particularly in addressing missing classes. Besides, latest works (Sarkar, Narang, and Rai 2020; Yang et al. 2021; Shuai et al. 2022; Zhang et al. 2022) mitigated the class imbalance, most of which modified the loss for specific classes or clients to rebalance intra- or inter-client imbalance. However, these inter-client re-balancing approaches involve potential privacy risks and demand additional communication and computation costs (Xiao et al. 2024b).

Inter-client imbalance on the server causes biased client updates, distorting its aggregation. For instance, in FedAvg (McMahan et al. 2017), averaging biased updates results in poor global gradient estimation (Su, Xu, and Yang 2023), slowing convergence and reducing accuracy. On the client

\*Corresponding author.

side, catastrophic forgetting (Babakniya et al. 2024) of rare or missing classes further contributes to biased updates. Furthermore, the FL system requires minimal information exchange, constrained communication, and flexible participation, which filter out or invalidate most CL and FL methods. For example, the missing class problem undermines the effectiveness of re-sampling and re-weighting in the FL system. Even modified loss functions fail to re-balance the client and reduce the update bias as the missing class is not present in the client dataset. From there, as depicted in Fig. 1, this work proposes a gradient alignment approach to cope with the aforementioned challenge, and the main contributions are three-fold:

- We prove that class imbalance in FL is fundamentally associated with asymmetric Type I and Type II errors as the gradient of the raw logits is composed of mismatched active and inactive ones corresponding to these errors.
- We propose a gradient alignment (GA) algorithm via label calibration to scale the active and inactive gradients, named FedGA, to eliminate error asymmetry (EA) as the first class-wise bias reduction algorithm free of extra privacy and communication concerns in FL.
- We show that FedGA is superior to five state-of-the-art algorithms in reducing EA and client update bias while improving convergence speed, accuracy, and F1 score over five benchmark datasets with a high degree of self-explainability and scalability for decentralized AI.

## Related Works

The class imbalance in FL shares similarities with CL but presents distinct challenges. While several studies have addressed that in CL (Elkan 2001; Chawla et al. 2002; He et al. 2008; Liu, Wu, and Zhou 2008), fewer have focused on FL, which are categorized into data- and model-level methods.

**Data-Level Approaches.** This category of approaches addresses sample imbalance mostly through random oversampling of the minority class or undersampling of the majority class (Liu, Wu, and Zhou 2008). Heuristic re-sampling methods (Tang and He 2015) target difficult minority examples, while the synthetic minority oversampling technique (SMOTE) (Chawla et al. 2002) and its derivatives generate synthetic minority samples to mitigate information loss and overfitting (He et al. 2008). In addition, generative adversarial network (GAN)-based methods (Ali-Gombe and Elyan 2019) were employed to produce synthetic minority samples.

**Model-Level Approaches.** Unlike data-level approaches, model-level approaches address the issue during training. Simple adjustments, *e.g.* altering class weights or modifying the decision threshold, have been proven to mitigate the issue (Elkan 2001). The use of specialized loss functions for class imbalance, *e.g.* focal loss (Lin et al. 2017) and class-balanced loss (Cui et al. 2019), further improves performance under label skew. Besides, ensemble learning (Feng, Huang, and Ren 2018), one-class learning (Lee, Park, and Im 2023), and transfer learning (Li et al. 2024) were promising solutions.

**FL-Specific Approaches.** At present, limited researches address this issue in FL, focusing on intra-client (local) and inter-client (global) imbalances. Several studies further explore inter-client imbalance as the mismatch between lo-

cal and global imbalances (Wang et al. 2021; Xiao and Wang 2021). Loss function-based approaches are commonly adopted in FL. Fed-focal loss (Sarkar, Narang, and Rai 2020) combines focal loss with client selection to improve minority class performance, while ratio loss (FedRL) (Wang et al. 2021) addresses global imbalance by introducing a ratio parameter to indicate imbalance levels, raising privacy concerns. Zhang et al. utilizes a modified softmax function for intra-client imbalance (Zhang et al. 2022) but does not fully cover the class-missing problem. Client selection methods (Yang et al. 2021), such as Astraea (Duan et al. 2020), balance clients into groups, but add complexity and privacy risks. BalanceFL (Shuai et al. 2022), a combination of knowledge distillation and other methods, addresses inter-client imbalance and missing classes, however, is not sufficiently generalizable. Dai et al. tackles data heterogeneity through class prototypes (Dai et al. 2023), also raising privacy issues. CLIMB (Shen et al. 2021) leverages loss constraints to minimize client update bias by capturing the mismatch between local and global imbalances, but involves transmitting dual variables and local models to the server.

## Asymmetric Error

### Types of Asymmetric Error

Inter-client imbalance is commonly deemed for producing biased updates from clients, thus compromising global model aggregation (Kim et al. 2024). Furthermore, the linear combination of biased updates results in an inaccurate estimation of the global gradient, thus hindering convergence (Varmo et al. 2022). Fig. 2 illustrates the divergence of models trained on locally imbalanced data across various clients, revealing significant disparities in their effects on different classes. This results in catastrophic forgetting (Babakniya et al. 2024), particularly for minority and absent classes. Consequently, aggregating these divergent and biased client models poses a substantial challenge at the global level, as the weighted average operation used for model aggregation does not accurately reflect actual performance of the models.

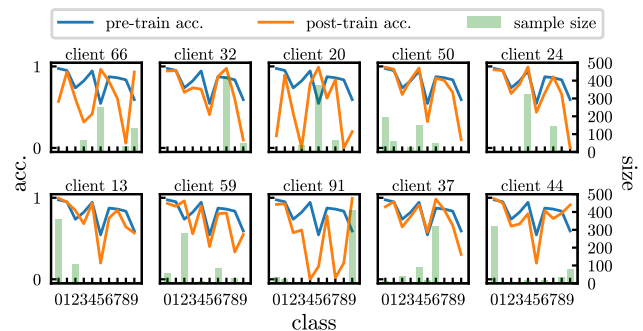


Figure 2: Class accuracy before and after local training with classical FedAvg on inter-client imbalanced MNIST. Each subplot corresponds to a random active client, showing sharp accuracy drops for rare and missing classes post-training.

Class imbalance leads to model bias for several reasons, notably inadequate sample size (Tao et al. 2024) and un-

derestimated loss (Xiao et al. 2024a). While data-level and algorithm-level approaches are employed to cope with this issue, label distribution and loss values do not directly measure model bias, making them insufficient for bias elimination. Instead of depending on input labels or class loss, we propose a direct measure of model bias, dubbed Error Asymmetry (EA), which is based on two types of errors. This measure informs a novel approach to effectively mitigate bias.

Typically, Type I error  $u_I$  and Type II error  $u_{II}$  refer to a false positive and a false negative, respectively. Practically, the error is commonly defined as the difference between the model prediction  $p$  and the ground-truth label  $y$ . Hence, these two types of errors can be written as:

$$\begin{cases} u_I = |p - 1| & (y = 1), \\ u_{II} = |p| & (y = 0). \end{cases} \quad (1)$$

### Measurable Error Asymmetry

Given an input data instance  $x$ , the corresponding ground-truth label  $y$ , and a binary classifier  $f_\theta$ , the prediction error  $u$  is expressed by  $|y - p|$  where  $p$  equals to  $f_\theta(x)$ . The prediction error of the minority class (*i.e.*  $u_I$ ) tends to be larger than that of the majority class (*i.e.*  $u_{II}$ ) since  $\mathbb{E}(u|y = 1) \gg \mathbb{E}(u|y = 0)$ . Indicating less confidence in the minority class, this aligns with the biased model achieving less competitive performance on the minority class.

Using an imbalanced MNIST (Deng 2012) binary subset containing  $N_0$  negative and  $N_1$  positive samples, we logged two types of errors during training, as shown in Fig. 3. Despite the imbalance ratios ( $r$ ), the  $u_I$  always converges to  $r$  times that of  $u_{II}$ . As such, we term the ratio of Type I and II errors in class imbalance as EA  $\mathcal{E}$  which is computed by  $u_I/u_{II}$ .

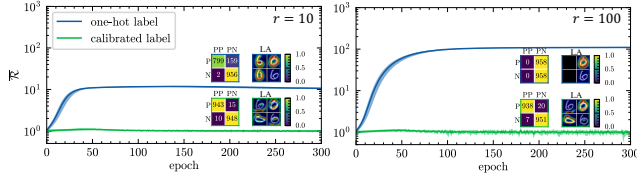


Figure 3: Mean error ratio between Type I to Type II error on an imbalanced binary (*e.g.* class ‘6’ and ‘0’) subset of the MNIST dataset with imbalance ratio  $r$  valued as 10 and 100. PP and PN represent predicted positive and negative, respectively. LA denotes layerwise attention. Noteworthy, FedGA (green) is equivalent to FedAvg (blue) when  $r$  equals 1. Best viewed in color and zoomed mode.

Apart from EA, the cumulative Type I and Type II errors always converge to 1, as the ratio of negative and positive samples is  $r$ . Equivalently,  $N_1\mathbb{E}(e|y = 1) \approx N_0\mathbb{E}(e|y = 0)$  holds for any  $r = \frac{N_0}{N_1}$  empirically. Diving into the gradient descent process, we discovered the cause of EA. Given the binary classifier with cross-entropy loss  $\mathcal{L}_{\text{BCE}}(x, y) = -y \log p - (1 - y) \log(1 - p)$  and sigmoid activation function  $\sigma(z) = \frac{1}{1 + e^{-z}}$  at the output layer, the gradient  $\delta$  of loss  $\mathcal{L}$  to raw logits  $z$  is  $\delta = \frac{\partial \mathcal{L}}{\partial z} = p - y$  according to the chain

rule. With a gradient descent step over the imbalanced dataset, the cumulative gradient is computed as:

$$\sum \delta = \underbrace{N_1(\overline{p^{(1)}} - 1)}_{\text{active gradient}} + \underbrace{N_0\overline{p^{(0)}}}_{\text{inactive gradient}}, \quad (2)$$

where  $\overline{p^{(1)}} = \mathbb{E}(p|y = 1)$  and  $\overline{p^{(0)}} = \mathbb{E}(p|y = 0)$  are the average predictions for positive and negative samples, respectively. In line with Eq. (1), it is clear the active gradient is  $N_i$  times the Type I error and the inactive gradient is  $N_j$  times the Type II error. As the optimization process aims to locate the global optimum and find the weights with zero gradient, the cumulative gradient in Eq. (2) always converges to zero. Thus, let Eq. (2) equals to zero, the EA is calculated as:

$$\mathcal{E} = \frac{1 - \overline{p^{(1)}}}{\overline{p^{(0)}}} \approx \frac{N_0}{N_1} = r. \quad (3)$$

### Bounded Error Asymmetry

Similar to binary classification with sigmoid activation function and BCE loss, the derivative of loss regarding raw logits in multi-class classification with softmax activation function and cross-entropy is  $\delta = \mathbf{p} - \mathbf{y}$ . This is the same as the binary case, except that  $\delta$ ,  $\mathbf{p}$ , and  $\mathbf{y}$  are vectors. Therefore, the above analysis on the gradient and EA can be generalized to multi-class problems. Concretely, given a gradient descent step in multi-class classification, the cumulative gradient is defined by:

$$\sum_D \delta_i = N_i \underbrace{(\overline{p_i^{(i)}} - 1)}_{u_I} + \sum_{j \neq i} \underbrace{(\overline{p_i^{(j)}})}_{u_{II}} N_j, \quad (4)$$

in which  $\overline{p_i^{(j)}} = \frac{1}{N_j} \sum_{y=j} f(x)_i$  is the average probability of predicting data with label  $j$  as class  $i$ .

**Definition 1** For a binary classifier trained with sigmoid activation function at the last layer and binary cross-entropy loss, or a multi-class classifier with softmax activation function at the last layer and cross-entropy loss, the EA is the ratio of Type I error to Type II error for the target class  $i$ :

$$\mathcal{E}(i) = \frac{1 - \overline{p_i^{(i)}}}{\sum_{j \neq i} \overline{p_i^{(j)}}}. \quad (5)$$

By setting Eq. (4) to zero, and simply scaling and rearranging the terms, we can solve for EA in different scenarios. When the dataset is balanced ( $N_i = N_j, \forall i, j$ ), the EA of all classes is close to 1. When the dataset is imbalanced ( $N_i \ll N_j, \exists i, \forall j \neq i$ ), the EA of the minority class  $i$  is larger than 1:

$$\begin{aligned} \mathcal{E}(i) &= \frac{N_i(1 - \overline{p_i^{(i)}})}{\sum_{j \neq i} N_j \overline{p_i^{(j)}}} \\ &\gg \frac{N_i(1 - \overline{p_i^{(i)}})}{\sum_{j \neq i} N_i \overline{p_i^{(j)}}} \\ &= 1. \end{aligned} \quad (6)$$

## Gradient Alignment via Label Calibration

The model’s bias toward the minority class is linked to EA and can be mitigated by aligning gradients to force the EA to 1. Over-sampling and under-sampling methods follow this gradient-based approach by scaling class samples. Re-sampling and re-weighting apply a weight  $\alpha_i$  to class  $i$ , ensuring  $\alpha_i N_i = \alpha_j N_j, \forall i, j$ . This weighting, applied to Eq. (4), eliminates the EA, setting it to 1.

Two limitations exist: re-sampling and re-weighting fail for missing classes, and weighting risks overfitting or underfitting. We address this with class-wise gradient alignment (GA), rescaling inactive gradients to match active ones by adjusting  $N_j$  to  $N_i$  in Eq. (4):

$$\sum_D \delta_i = N_i \overline{u}_1 + \sum_{j \neq i} N_j \overline{u}_1. \quad (7)$$

Aligned gradients equalize Type I and II errors. For missing class  $i$ , the inactive gradient is rescaled to zero, preventing forgetting and bias. GA uses calibrated label embedding, replacing one-hot labels  $\mathbf{1}(\cdot)$  with  $\mathbb{C}(\cdot)$ . With calibrated label  $\mathbf{q}^{(i)}$ , Eq. (4) becomes:

$$\sum_D \delta_i = N_i (\overline{p}_i^{(i)} - \mathbf{q}_i^{(i)}) + \sum_{j \neq i} N_j (\overline{p}_i^{(j)} - \mathbf{q}_i^{(j)}). \quad (8)$$

To achieve the aligned gradient as in Eq. (7), we have  $N_j (\overline{p}_i^{(j)} - \mathbf{q}_i^{(j)}) = N_i \overline{p}_i^{(j)}$ . By solving this, the calibrated label for inactive class  $k \neq i$  is:

$$\mathbf{q}_i^{(j)} = \frac{N_j - N_i \overline{p}_i^{(j)}}{N_j}. \quad (9)$$

As such, the calibrated label for the imbalanced dataset can be summarized as:

$$\mathbb{C}_i(j) = \begin{cases} 1 & \text{if } j = i, \\ \frac{N_j - N_i \overline{p}_i^{(j)}}{N_j} & \text{otherwise.} \end{cases} \quad (10)$$

By combining Eqs. (5), (8), and (10) and setting Eq.(9) to zero, GA eliminates EA, except for missing classes where the gradient is zero, preventing bias and class forgetting. Unlike under-sampling, GA mutes only the missing class gradient, preserving learning. FedGA is summarized in Algorithm 1.

## Experiments

To evaluate the proposed GA algorithm with label calibration, we conducted four experiments. Along with FedAvg, we included FedProx (Li et al. 2020) as a baseline. Three variants of FedAvg, CLIMB, FedRL, and FedNTD, were compared on five benchmark datasets: MNIST (Deng 2012), CIFAR-10, CIFAR-100 (Krizhevsky 2009), SVHN (Netzer et al. 2011), and Tiny-ImageNet (Le and Yang 2015), chosen for their varying data heterogeneity and classification difficulty. Each dataset was split among 100 clients, with 10 randomly selected each round. Additional results are in the *supplementary materials*.

---

### Algorithm 1: Federated Learning with Gradient Alignment (FedGA)

---

#### ServerExecute:

- 1: **for** round  $t \leftarrow 0$  to  $T - 1$  **do**
- 2:   select  $K$  out of  $P$  clients randomly
- 3:   **for**  $k \leftarrow 0$  to  $K - 1$  **synchronously do**
- 4:      $w_{t+1}^k \leftarrow \text{ClientUpdate}(w_t)$
- 5:   **end for**
- 6:   aggregate to  $w_{t+1}$    ▷ debiased model aggregation
- 7: **end for**

#### ClientUpdate:

- 1: load global model  $w$
  - 2: **for**  $e \leftarrow 1, E$  **do**
  - 3:   **for**  $\mathbf{x}, \mathbf{y} \in S^{(k)}$  **do**
  - 4:      $\mathbf{p} = f(\mathbf{x})$    ▷ batch prediction
  - 5:      $\mathbf{q} = \mathbb{C}(\mathbf{y}, \mathbf{p})$    ▷ batch calibrated label, Eq. (10)
  - 6:      $l = \mathcal{L}(\mathbf{q}, \mathbf{p})$
  - 7:     update  $w$    ▷ debiased model update
  - 8:   **end for**
  - 9: **end for**
  - 10: feedback updated  $w$  to server
- 

## Inter-client Imbalance Impact

To assess inter-client imbalance in FL, we conducted an ablation study comparing FedGA and FedAvg on client datasets sampled by Dirichlet( $\alpha$ ). Fig. 4 reveals that FedGA’s accuracy is less impacted by  $\alpha$  than FedAvg, where smaller  $\alpha$  increases imbalance and reduces performance.

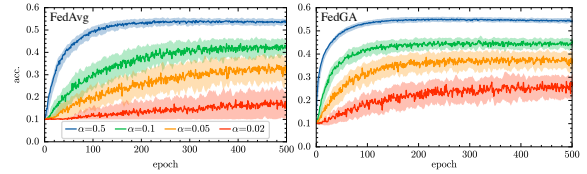


Figure 4: Comparative accuracy of FedAvg and FedGA on CIFAR-10 with four inter-client imbalance levels. FedGA converges much faster than FedAvg at each  $\alpha$ .

## Measurable EA Reduction

Given Definition 1, client EA is measured for all algorithms during training. The EA ratio  $\mathcal{E}_{\max}/\mathcal{E}_{\min}$  tracks class imbalance every ten iterations. Fig. 5 shows FedGA’s average

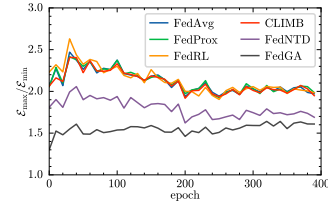


Figure 5: The average EA ratio of ten active clients on inter-client imbalance CIFAR-10 during the training phase.

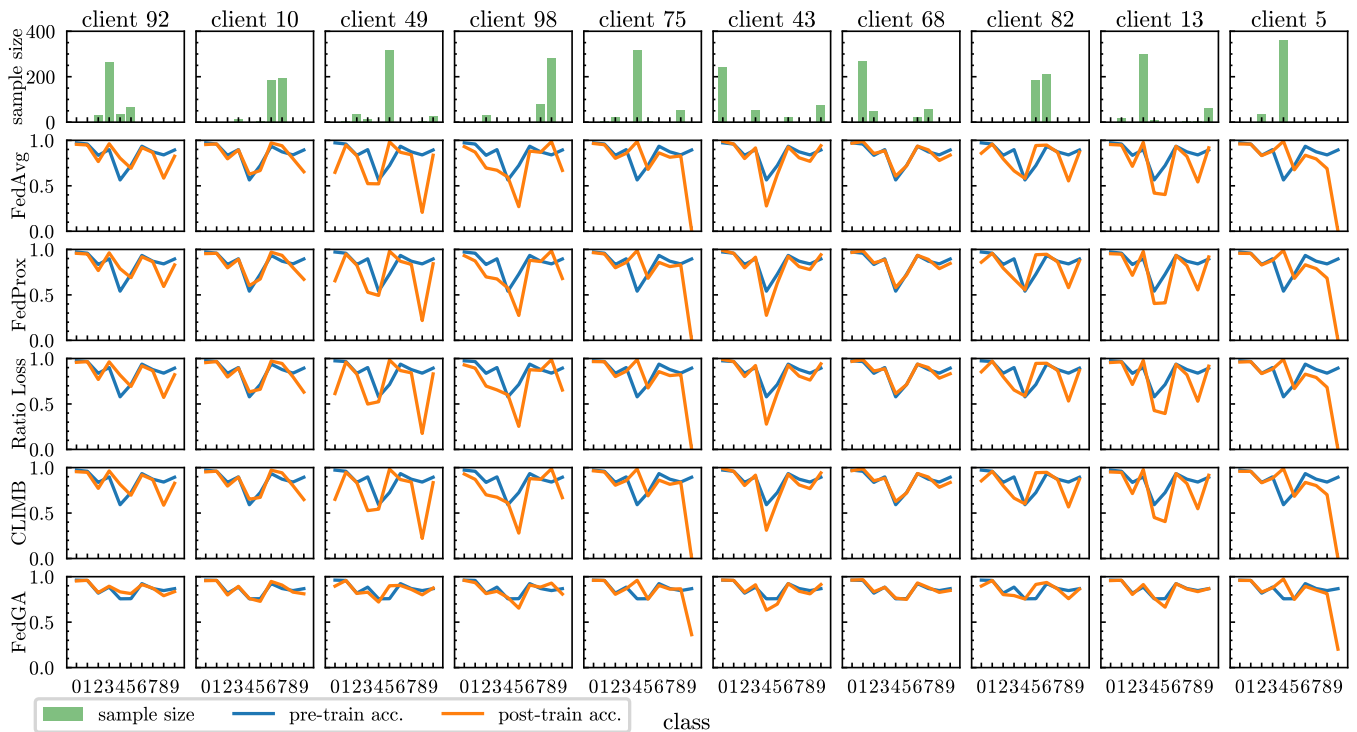


Figure 6: Sample distribution as well as pre-train and post-train accuracies of 10 random active clients executing five FL algorithms on inter-client imbalance MNIST dataset. Best viewed in color and zoomed mode.

EA ratio is consistently lower than others, indicating GA reduces EA, as a ratio near 1 implies balanced EA across classes.

### Quantifiable Model Bias Reduction

We measure class-wise accuracy before and after local training to evaluate the bias reduction of the approaches selected for systematic comparisons. The test dataset employed is a standalone balanced dataset. Fig. 6 illustrates the average accuracy of 10 active clients before and after local training, along with the client sample distribution. Notably, GA exhibits significantly less catastrophic forgetting on the rare and missing classes compared to the other four algorithms. Additionally, the accuracy of GA before local training is less biased than the other algorithms, suggesting that GA aggregates into a more balanced global model in the last iteration.

### Overall Classification Comparisons

A balanced test dataset is used to evaluate the performance of the selected FL re-balancing algorithms, ensuring fair assessment across all classes. Overall accuracy remains a key criterion for model selection, while the multi-class F1 score is calculated to provide a more comprehensive evaluation of performance across imbalanced classes. To ensure statistical reliability, each experiment is repeated 20 times with random seeds (from 0 to 19), reducing the influence of variability and ensuring consistent results (Wang et al. 2024a).

The average accuracy and F1 score, along with the corresponding standard deviation, are detailed in Tab.1. Across ex-

periments conducted on various datasets and under different levels of class imbalance, GA consistently demonstrates superior performance in both accuracy and F1 score compared to the other four algorithms. This highlights the effectiveness of GA in addressing data heterogeneity and maintaining robust performance across diverse scenarios. Additionally, the smaller standard deviation observed in GA’s results indicates greater stability and reliability, underscoring its ability to produce consistent outcomes across multiple runs. Notably, for the SVHN dataset (Netzer et al. 2011) with  $\alpha = 0.1$  and  $0.5$ , GA exhibits a slightly larger standard deviation. This deviation, however, reflects the instability of the baseline algorithms, which fail to converge within the allocated number of global iterations, rather than a limitation of GA. This reinforces GA’s resilience in challenging conditions where other algorithms struggle to achieve convergence.

On the simple MNIST (Deng 2012) dataset, GA’s performance is slightly better than that of other algorithms. As  $\alpha$  decreases from 0.5 to 0.05, the inter-client imbalance level increases. The performance advantage of GA over other algorithms expands with the increased inter-client imbalance. For the challenging tasks of SVHN (Netzer et al. 2011) and CIFAR-10 (Krizhevsky 2009), GA significantly outperforms the other algorithms. For instance, GA achieves 72% accuracy on SVHN with  $\alpha = 0.1$ , while the others remain below 20%. Even when  $\alpha = 0.05$ , GA still achieves 28.9% accuracy on SVHN, outperforming the others, which hover around 10%, akin to random guessing. In addition to the average accuracy and F1 score, the convergence speed stands out

Dataset	$\alpha$	Met.	FedAvg	FedProx	FedRL	CLIMB	FedNTD	FedGA
MNIST	0.05	F1	0.799 (0.020)	0.799 (0.020)	0.837 (0.013)	0.803 (0.020)	0.810 (0.020)	<b>0.852 (0.013)</b>
		acc.	0.812 (0.016)	0.812 (0.016)	0.845 (0.011)	0.815 (0.016)	0.821 (0.018)	<b>0.859 (0.011)</b>
	0.1	F1	0.841 (0.006)	0.841 (0.006)	0.873 (0.008)	0.843 (0.006)	0.856 (0.004)	<b>0.880 (0.001)</b>
		acc.	0.849 (0.005)	0.849 (0.005)	0.877 (0.007)	0.852 (0.004)	0.863 (0.004)	<b>0.885 (0.001)</b>
	0.5	F1	0.904 (0.001)	0.903 (0.001)	0.916 (0.003)	0.904 (0.002)	0.912 (0.002)	<b>0.917 (0.001)</b>
		acc.	0.905 (0.002)	0.905 (0.002)	0.917 (0.003)	0.906 (0.002)	0.914 (0.003)	<b>0.918 (0.001)</b>
1	F1	0.913 (0.001)	0.913 (0.001)	<b>0.924 (0.006)</b>	0.913 (0.001)	0.917 (0.001)	0.921 (0.001)	
	acc.	0.914 (0.001)	0.914 (0.001)	<b>0.925 (0.006)</b>	0.914 (0.001)	0.919 (0.001)	0.922 (0.001)	
10	F1	0.923 (0.001)	0.923 (0.001)	<b>0.934 (0.004)</b>	0.923 (0.001)	0.924 (0.001)	0.923 (0.001)	
	acc.	0.924 (0.001)	0.924 (0.001)	<b>0.934 (0.004)</b>	0.924 (0.001)	0.925 (0.001)	0.925 (0.001)	
CIFAR-10	0.05	F1	0.428 (0.017)	0.424 (0.014)	0.413 (0.013)	0.428 (0.015)	0.413 (0.011)	<b>0.443 (0.006)</b>
		acc.	0.446 (0.016)	0.443 (0.011)	0.427 (0.012)	0.446 (0.014)	0.430 (0.010)	<b>0.451 (0.006)</b>
	0.1	F1	0.440 (0.022)	0.441 (0.021)	0.426 (0.017)	0.445 (0.021)	0.448 (0.019)	<b>0.469 (0.011)</b>
		acc.	0.459 (0.019)	0.460 (0.017)	0.440 (0.015)	0.463 (0.017)	0.464 (0.015)	<b>0.477 (0.010)</b>
	0.5	F1	0.520 (0.005)	0.518 (0.007)	0.497 (0.017)	0.518 (0.004)	0.525 (0.003)	<b>0.529 (0.007)</b>
		acc.	0.525 (0.004)	0.523 (0.006)	0.500 (0.017)	0.523 (0.003)	0.529 (0.003)	<b>0.532 (0.006)</b>
1	F1	0.537 (0.017)	0.535 (0.016)	0.479 (0.017)	0.536 (0.015)	0.534 (0.009)	<b>0.544 (0.006)</b>	
	acc.	0.541 (0.017)	0.539 (0.016)	0.485 (0.016)	0.540 (0.014)	0.538 (0.010)	<b>0.547 (0.005)</b>	
10	F1	0.559 (0.005)	0.559 (0.006)	0.373 (0.205)	0.559 (0.007)	0.549 (0.009)	<b>0.565 (0.002)</b>	
	acc.	0.561 (0.005)	0.561 (0.006)	0.397 (0.172)	0.561 (0.006)	0.551 (0.009)	<b>0.567 (0.002)</b>	
CIFAR-100	0.05	F1	0.135 (0.016)	0.157 (0.018)	<b>0.197 (0.021)</b>	0.117 (0.009)	0.162 (0.022)	0.154 (0.018)
		acc.	0.149 (0.017)	0.175 (0.021)	<b>0.211 (0.023)</b>	0.131 (0.010)	0.180 (0.025)	0.167 (0.018)
	0.1	F1	0.207 (0.002)	0.208 (0.004)	0.203 (0.018)	0.197 (0.007)	0.224 (0.011)	<b>0.227 (0.007)</b>
		acc.	0.223 (0.003)	0.225 (0.005)	0.220 (0.016)	0.212 (0.009)	0.237 (0.013)	<b>0.241 (0.007)</b>
	0.5	F1	0.294 (0.003)	0.297 (0.002)	0.197 (0.006)	0.294 (0.003)	<b>0.299 (0.006)</b>	0.299 (0.003)
		acc.	0.304 (0.003)	0.306 (0.001)	0.222 (0.006)	0.304 (0.003)	<b>0.309 (0.004)</b>	0.306 (0.003)
1	F1	0.323 (0.008)	0.321 (0.008)	0.205 (0.002)	0.322 (0.006)	0.318 (0.008)	<b>0.327 (0.008)</b>	
	acc.	0.329 (0.008)	0.327 (0.010)	0.225 (0.004)	0.328 (0.008)	0.323 (0.008)	<b>0.330 (0.009)</b>	
10	F1	0.339 (0.013)	0.336 (0.008)	0.177 (0.007)	0.334 (0.013)	0.331 (0.003)	<b>0.342 (0.005)</b>	
	acc.	0.346 (0.012)	0.343 (0.007)	0.198 (0.009)	0.342 (0.011)	0.340 (0.004)	<b>0.347 (0.006)</b>	
SVHN	0.05	F1	0.760 (0.076)	0.772 (0.057)	0.794 (0.023)	0.770 (0.050)	0.766 (0.053)	<b>0.801 (0.007)</b>
		acc.	0.776 (0.071)	0.787 (0.054)	0.808 (0.023)	0.785 (0.048)	0.782 (0.052)	<b>0.815 (0.008)</b>
	0.1	F1	0.817 (0.015)	0.817 (0.014)	0.738 (0.252)	0.818 (0.014)	0.814 (0.010)	<b>0.820 (0.008)</b>
		acc.	0.831 (0.013)	0.831 (0.013)	0.758 (0.228)	0.831 (0.012)	0.828 (0.009)	<b>0.834 (0.007)</b>
	0.5	F1	0.832 (0.009)	0.667 (0.365)	0.494 (0.371)	0.673 (0.365)	0.829 (0.012)	<b>0.838 (0.005)</b>
		acc.	0.844 (0.008)	0.690 (0.341)	0.531 (0.342)	0.696 (0.341)	0.842 (0.010)	<b>0.851 (0.005)</b>
1	F1	<b>0.843 (0.011)</b>	0.842 (0.007)	0.424 (0.362)	0.840 (0.010)	0.839 (0.005)	0.840 (0.009)	
	acc.	<b>0.856 (0.010)</b>	0.854 (0.007)	0.469 (0.329)	0.852 (0.009)	0.853 (0.005)	0.853 (0.009)	
10	F1	0.848 (0.006)	0.848 (0.006)	0.018 (0.002)	<b>0.850 (0.006)</b>	0.844 (0.009)	0.848 (0.007)	
	acc.	0.860 (0.006)	0.861 (0.006)	0.102 (0.011)	<b>0.862 (0.005)</b>	0.857 (0.008)	0.861 (0.007)	
Tiny-ImageNet	0.05	F1	0.055 (0.015)	0.085 (0.010)	<b>0.091 (0.011)</b>	0.043 (0.013)	0.084 (0.008)	0.065 (0.015)
		acc.	0.075 (0.015)	0.106 (0.010)	<b>0.110 (0.007)</b>	0.057 (0.013)	0.103 (0.008)	0.086 (0.015)
	0.1	F1	0.114 (0.011)	0.119 (0.003)	0.102 (0.024)	0.103 (0.023)	0.123 (0.017)	<b>0.124 (0.008)</b>
		acc.	0.134 (0.011)	0.142 (0.002)	0.120 (0.024)	0.120 (0.024)	0.139 (0.016)	<b>0.144 (0.007)</b>
	0.5	F1	0.174 (0.016)	0.179 (0.014)	0.052 (0.020)	0.177 (0.010)	<b>0.195 (0.006)</b>	0.193 (0.012)
		acc.	0.195 (0.015)	0.199 (0.012)	0.077 (0.020)	0.196 (0.008)	<b>0.212 (0.004)</b>	0.209 (0.012)
1	F1	0.206 (0.013)	0.205 (0.009)	0.039 (0.016)	0.201 (0.009)	0.210 (0.010)	<b>0.213 (0.009)</b>	
	acc.	0.222 (0.014)	0.221 (0.010)	0.061 (0.017)	0.216 (0.009)	0.223 (0.011)	<b>0.225 (0.009)</b>	
10	F1	0.236 (0.007)	0.235 (0.005)	0.053 (0.015)	0.224 (0.007)	0.239 (0.004)	<b>0.243 (0.004)</b>	
	acc.	0.247 (0.008)	0.246 (0.004)	0.079 (0.016)	0.235 (0.007)	0.249 (0.005)	<b>0.251 (0.005)</b>	

Table 1: Validation accuracy and F1 score of different FL algorithms on MNIST, CIFAR-10, CIFAR-100, SVHN and Tiny-ImageNet with different levels of heterogeneity. The results are averaged over five independent runs with standard deviation reported in parentheses. The best results for each setting  $\alpha$  are marked in bold.

as a strength of GA. As illustrated in Fig. 7, GA converges significantly faster than the other algorithms. When considering the time it takes to reach 90% of the final accuracy, GA is three times faster than the other algorithms in the selected experiment.

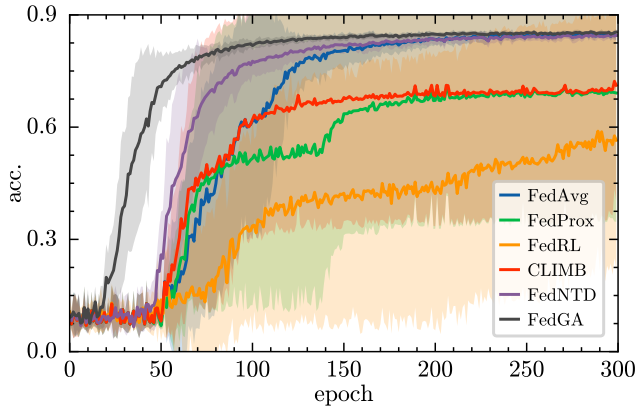


Figure 7: The accuracy curve of GA and other algorithms on an inter-client imbalanced SVHN dataset sampled with  $\alpha = 0.5$ . The shaded area denotes the standard deviation over five independent runs.

## Conclusion

This paper investigates the model bias caused by FL inter-client imbalance from a novel perspective of the gradient. It identifies the asymmetric Type I and Type II errors in class imbalance and establishes a connection between the gradient of loss and the raw logits. The proposed GA approach, *i.e.* FedGA, involves label calibration to align active and inactive gradients, ultimately eliminating the EA. Extensive experimental results confirm the efficacy and efficiency of the FedGA in eliminating EA and reducing client bias. Experimental results also inspire further investigations on the optimal sample selection (Cui et al. 2019) for more robust label calibration, as well as GA extension for a wider spectrum of downstream tasks.

## Acknowledgements

This work was supported by the EPSRC Early Career Researchers International Collaboration Grants (EP/Y002539/1) and the National Natural Science Foundation for Young Scientists of China [62206239]. The computations described in this research were performed using the Baskerville Tier 2 HPC service (<https://www.baskerville.ac.uk/>). Baskerville was funded by the EPSRC and UKRI through the World Class Labs scheme (EP/T022221/1) and the Digital Research Infrastructure programme (EP/W032244/1) and is operated by Advanced Research Computing at the University of Birmingham. Chenguang Xiao is partially supported by the Chinese Scholarship Council.

## References

Ali-Gombe, A.; and Elyan, E. 2019. MFC-GAN: Class-imbalanced dataset classification using multiple fake class

generative adversarial network. *Neurocomputing*, 361: 212–221.

Babakniya, S.; Fabian, Z.; He, C.; Soltanolkotabi, M.; and Avestimehr, S. 2024. A data-free approach to mitigate catastrophic forgetting in federated class incremental learning for vision tasks. In *Advances in Neural Information Processing Systems*.

Chawla, N. V.; Bowyer, K. W.; Hall, L. O.; and Kegelmeyer, W. P. 2002. SMOTE: synthetic minority over-sampling technique. *Journal of Artificial Intelligence Research*, 16: 321–357.

Cui, Y.; Jia, M.; Lin, T.-Y.; Song, Y.; and Belongie, S. 2019. Class-balanced loss based on effective number of samples. In *IEEE/CVF Conference on Computer Vision and Pattern Recognition*, 9268–9277.

Dai, Y.; Chen, Z.; Li, J.; Heinecke, S.; Sun, L.; and Xu, R. 2023. Tackling data heterogeneity in federated learning with class prototypes. In *AAAI Conference on Artificial Intelligence*, 7314–7322.

Deng, L. 2012. The mnist database of handwritten digit images for machine learning research. *IEEE Signal Processing Magazine*, 29(6): 141–142.

Duan, M.; Liu, D.; Chen, X.; Liu, R.; Tan, Y.; and Liang, L. 2020. Self-balancing federated learning with global imbalanced data in mobile systems. *IEEE Transactions on Parallel and Distributed Systems*, 32(1): 59–71.

Elkan, C. 2001. The foundations of cost-sensitive learning. In *International Joint Conference on Artificial Intelligence*, 973–978.

Feng, W.; Huang, W.; and Ren, J. 2018. Class imbalance ensemble learning based on the margin theory. *Applied Sciences*, 8(5): 815.

He, H.; Bai, Y.; Garcia, E. A.; and Li, S. 2008. ADASYN: Adaptive synthetic sampling approach for imbalanced learning. In *IEEE International Joint Conference on Neural Networks*, 1322–1328.

Kim, T.; Lin, E.; Lee, J.; Lau, C.; and Mugunthan, V. 2024. Navigating Data Heterogeneity in Federated Learning: A Semi-Supervised Approach for Object Detection. In *Advances in Neural Information Processing Systems*.

Krizhevsky, A. 2009. Learning Multiple Layers of Features from Tiny Images. Technical Report TR-2009, University of Toronto.

Le, Y.; and Yang, X. 2015. Tiny imagenet visual recognition challenge. *CS 231N*, 7(7): 3.

Lee, H.-H.; Park, S.; and Im, J. 2023. Resampling approach for one-Class classification. *Pattern Recognition*, 143: 109731.

Li, T.; Sahu, A. K.; Zaheer, M.; Sanjabi, M.; Talwalkar, A.; and Smith, V. 2020. Federated optimization in heterogeneous networks. *Proceedings of Machine Learning and Systems*, 2: 429–450.

Li, Z.; Ma, J.; Wu, J.; Wong, P. K.; Wang, X.; and Li, X. 2024. A Gated Recurrent Generative Transfer Learning Network for Fault Diagnostics Considering Imbalanced Data and Variable

- Working Conditions. *IEEE Transactions on Neural Networks and Learning Systems*.
- Lin, T.-Y.; Goyal, P.; Girshick, R.; He, K.; and Dollár, P. 2017. Focal loss for dense object detection. In *IEEE International Conference on Computer Vision*, 2980–2988.
- Liu, X.-Y.; Wu, J.; and Zhou, Z.-H. 2008. Exploratory under-sampling for class-imbalance learning. *IEEE Transactions on Systems, Man, and Cybernetics, Part B (Cybernetics)*, 39(2): 539–550.
- McMahan, B.; Moore, E.; Ramage, D.; Hampson, S.; and y Arcas, B. A. 2017. Communication-efficient learning of deep networks from decentralized data. In *Artificial Intelligence and Statistics*, 1273–1282.
- Netzer, Y.; Wang, T.; Coates, A.; Bissacco, A.; Wu, B.; Ng, A. Y.; et al. 2011. Reading digits in natural images with unsupervised feature learning. In *Advances in Neural Information Processing Systems*.
- Pei, J.; Liu, W.; Li, J.; Wang, L.; and Liu, C. 2024. A Review of Federated Learning Methods in Heterogeneous scenarios. *IEEE Transactions on Consumer Electronics*, 1–19.
- Sarkar, D.; Narang, A.; and Rai, S. 2020. Fed-focal loss for imbalanced data classification in federated learning. In *International Joint Conference on Artificial Intelligence Work*.
- Shen, Z.; Cervino, J.; Hassani, H.; and Ribeiro, A. 2021. An agnostic approach to federated learning with class imbalance. In *International Conference on Learning Representations*.
- Shi, J.; Zheng, S.; Yin, X.; Lu, Y.; Xie, Y.; and Qu, Y. 2024. CLIP-Guided Federated Learning on Heterogeneity and Long-Tailed Data. In *AAAI Conference on Artificial Intelligence*, 14955–14963.
- Shuai, X.; Shen, Y.; Jiang, S.; Zhao, Z.; Yan, Z.; and Xing, G. 2022. BalanceFL: Addressing class imbalance in long-tail federated learning. In *ACM/IEEE International Conference on Information Processing in Sensor Networks*, 271–284.
- Su, L.; Xu, J.; and Yang, P. 2023. A non-parametric view of FedAvg and FedProx: beyond stationary points. *Journal of Machine Learning Research*, 24(203): 1–48.
- Tang, B.; and He, H. 2015. ENN: Extended nearest neighbor method for pattern recognition [research frontier]. *IEEE Computational Intelligence Magazine*, 10(3): 52–60.
- Tao, X.; Zhang, X.; Zheng, Y.; Qi, L.; Fan, Z.; and Huang, S. 2024. A MeanShift-guided oversampling with self-adaptive sizes for imbalanced data classification. *Information Sciences*, 672: 120699.
- Varno, F.; Saghay, M.; Rafiee Sevyeri, L.; Gupta, S.; Matwin, S.; and Havaei, M. 2022. Adabest: Minimizing client drift in federated learning via adaptive bias estimation. In *European Conference on Computer Vision*, 710–726.
- Wang, G.; Gu, B.; Zhang, Q.; Li, X.; Wang, B.; and Ling, C. X. 2024a. A unified solution for privacy and communication efficiency in vertical federated learning. *Advances in Neural Information Processing Systems*.
- Wang, L.; Xu, S.; Wang, X.; and Zhu, Q. 2021. Addressing class imbalance in federated learning. In *AAAI Conference on Artificial Intelligence*, 10165–10173.
- Wang, M.; Bodonhelyi, A.; Bozkir, E.; and Kasneci, E. 2024b. TurboSVM-FL: Boosting Federated Learning through SVM Aggregation for Lazy Clients. In *AAAI Conference on Artificial Intelligence*.
- Wang, S.; Fu, Y.; Li, X.; Lan, Y.; Gao, M.; et al. 2024c. DFRD: Data-Free Robustness Distillation for Heterogeneous Federated Learning. In *Advances in Neural Information Processing Systems*.
- Wu, N.; Yu, L.; Yang, X.; Cheng, K.-T.; and Yan, Z. 2023. FedIIC: Towards robust federated learning for class-imbalanced medical image classification. In *International Conference on Medical Image Computing and Computer-Assisted Intervention*, 692–702.
- Wu, X.; Sun, J.; Hu, Z.; Zhang, A.; and Huang, H. 2024. Solving a class of non-convex minimax optimization in federated learning. In *Advances in Neural Information Processing Systems*.
- Xiao, C.; and Wang, S. 2021. An experimental study of class imbalance in federated learning. In *IEEE Symposium Series on Computational Intelligence*, 1–7.
- Xiao, C.; and Wang, S. 2023. Triplets oversampling for class imbalanced federated datasets. In *Springer Joint European Conference on Machine Learning and Knowledge Discovery in Databases*, 368–383.
- Xiao, Y.; Zhang, Q.; Tang, F.; Wang, R.; Li, Q.; and Wang, G. 2024a. Cycle-Fed: A Double-Confidence Unlabeled Data Augmentation Method Based on Semisupervised Federated Learning. *IEEE Transactions on Mobile Computing*.
- Xiao, Z.; Chen, Z.; Liu, S.; Wang, H.; Feng, Y.; Hao, J.; Zhou, J. T.; Wu, J.; Yang, H.; and Liu, Z. 2024b. Fed-grab: Federated long-tailed learning with self-adjusting gradient balancer. In *Advances in Neural Information Processing Systems*.
- Yang, M.; Wang, X.; Zhu, H.; Wang, H.; and Qian, H. 2021. Federated learning with class imbalance reduction. In *IEEE European Signal Processing Conference*, 2174–2178.
- Yazdinejad, A.; Dehghantanha, A.; Karimipour, H.; Srivastava, G.; and Parizi, R. M. 2024. A Robust Privacy-Preserving Federated Learning Model Against Model Poisoning Attacks. *IEEE Transactions on Information Forensics and Security*, 19: 6693–6708.
- Zhang, J.; Li, Z.; Li, B.; Xu, J.; Wu, S.; Ding, S.; and Wu, C. 2022. Federated learning with label distribution skew via logits calibration. In *International Conference on Machine Learning*, 26311–26329.
- Zhang, J.; Liu, Y.; Hua, Y.; and Cao, J. 2024. An Upload-Efficient Scheme for Transferring Knowledge From a Server-Side Pre-trained Generator to Clients in Heterogeneous Federated Learning. In *IEEE/CVF Conference on Computer Vision and Pattern Recognition*, 12109–12119.
- Zuo, Z.; Li, J.; Wei, B.; Yang, L.; Chao, F.; and Naik, N. 2019. Adaptive Activation Function Generation for Artificial Neural Networks through Fuzzy Inference with Application in Grooming Text Categorisation. In *IEEE International Conference on Fuzzy Systems*, 1–6.



Zuo, Z.; Smith, J.; Stonehouse, J.; and Obara, B. 2024. Robust and Explainable Fine-Grained Visual Classification with Transfer Learning: A Dual-Carriageway Framework. In *IEEE/CVF Conference on Computer Vision and Pattern Recognition Workshops*.

Zuo, Z.; Watson, M.; Budgen, D.; Hall, R.; Kennelly, C.; and Al Moubayed, N. 2021. Data Anonymization for Pervasive Health Care: Systematic Literature Mapping Study. *JMIR Medical Informatics*, 9(10): e29871.